

Dynamic critical behavior of the Landau-Peierls fluctuations: Scaling form of the dynamic density autocorrelation function for smectic-A films

A. Poniewierski and Robert Hołyst

Institute of Physical Chemistry and College of Science, Polish Academy of Sciences, Kasprzaka 44/52, 01-224 Warsaw, Poland

A. C. Price and L. B. Sorensen

Department of Physics, University of Washington, Seattle, Washington 98195

(Received 17 July 1998)

In this paper, we study the dynamic density autocorrelation function $G(\mathbf{r}, t)$ for smectic-A films in the layer sliding geometry. We first postulate a scaling form for G , and then we show that our postulated scaling form holds by comparing the scaling predictions with detailed numerical calculations. We find some deviations from the scaling form only for very thin films. For thick films, we find a region of a bulklike behavior, where the dynamics is characterized by the same static critical exponent η , which was originally introduced by Caillé [C. R. Acad. Sci. Ser. B **274**, 891 (1972)]. In the limit of very large distance perpendicular to the layer normal, or in the limit of very long time, we find that the decay of G is governed by the surface exponent $\chi = k_B T q_z^2 / (4\pi\gamma)$, where γ is the surface tension and the wave-vector component q_z satisfies the Bragg condition. We also find an intermediate perpendicular distance regime in which the decay of G is governed by the time-dependent exponent $\chi \exp(-t/\tau_0)$, where the relaxation time is given by $\tau_0 = \eta_3(Ld)/(2\gamma)$, where η_3 is the layer sliding viscosity, and Ld is the film thickness. [S1063-651X(99)03403-0]

PACS number(s): 61.30.Cz, 83.70.Jr

I. INTRODUCTION

Systems that are precisely at their lower marginal dimensionality (LMD) provide us with a unique opportunity to study the influence of the technically divergent Landau-Peierls thermal fluctuations on the correlation functions in these systems. Mother Nature has only given us two classes of systems that we can produce that are precisely at lower marginal dimension in three dimensions. We can study the correlation functions in these two classes of systems from the atomic scale up to the macroscopic scale. The first class of LMD systems consists of the fluid (i.e., both liquid and hexatic) smectic liquid crystals—namely, the smectic-A, smectic-C, hexatic-B, smectic-F, and smectic-I phases. The second class of LMD systems consists of the two-dimensional crystals. The specific feature that the three-dimensional liquid crystal class has in common with the two-dimensional crystal class is that, if the thermal fluctuations were any stronger, they would destroy the phase, or, equivalently, move the phase transition temperature to zero degrees. LMD occurs at three dimensions for these liquid crystals because of their unusual elasticity—they have more violent thermal fluctuations than three-dimensional crystals! The thermal fluctuations in two-dimensional crystals are comparably violent, and also destroy the long-range order that would be present in the absence of the thermal fluctuations. The special order in systems that are precisely at their LMD—and consequently do not have long-range order, but still have the same special kind of order that is found in normal systems precisely at their critical points—is called quasi-long-range order, or algebraic order—so named because the correlation functions decay algebraically in space.

Because of the uniqueness of the LMD phases, and because of their direct relevance to our modern understanding

of phase transitions via the renormalization group formalism, they have been extensively studied theoretically [1], and experimentally [2]. However, almost all of this first round of theoretical and experimental work was focused only on the static critical behavior of these two classes of systems. This body of theoretical and experimental work has established that the spatial decay of the static correlations is algebraic. But what about the temporal decay of the correlations? How do they decay? What are the theoretical predictions, and what do the experiments say? We answer the first half of this question (i.e., the half about theory) in this paper by presenting the space and time scaling form of the density autocorrelation function. We hope to answer the second half experimentally in the near future. So, our first goal is to extend both the theory and the experiments to include the dynamic critical phenomena in the liquid crystal systems.

Another very important issue, which was not investigated in detail by the first theoretical and experimental work, concerns the effects of finite size on the dynamics of real (and therefore finite) experimental systems. The theoretical algebraic divergence of the correlation functions only occurs in the thermodynamic limit—and it is clearly impossible to do experiments on infinite samples! How does the size of the system come into the problem? How big must we make our sample so that we will see the bulk behavior? Can we ever achieve this limit? How small must we make it before we see the surface effects? Can we ever achieve this limit? What is the right theory for finite-size samples with real surfaces? How does the surface tension come into the problem? What sets the relaxation time scale in realizable experiments? We answer these questions in this paper. So, our second goal is to extend both the theory and the experiments to include the effects of finite size on the dynamic critical phenomena in the liquid crystal systems.

The fluid smectic liquid crystals have a layered structure,

with two-dimensional fluidlike order within the layers, and with a special kind of one-dimensional translational order along the layering direction. The long-range order which would be present at zero temperature (even for infinite size systems), is destroyed by the effect of the Landau-Peierls thermal fluctuations when the system size tends to infinity (at any nonzero temperature). This results in an algebraic decay of the density autocorrelation function. As noted above, the corresponding Landau-Peierls static critical behavior has been studied both theoretically [1] and experimentally [2]. More recent work has also been devoted to understanding the effects of finite system size on the smectic layer fluctuations in smectic liquid crystals [3–9]. We also note a closely related work of Lei, Safinya, and Bruinsma *et al.* [10] on lyotropic lamellar phases. However, this early finite-size work also focused only on the static critical behavior.

To go beyond the static description of the correlations in smectic-*A* liquid crystals, it is necessary to study the hydrodynamics of the smectic-*A* phase. The full hydrodynamic behavior of smectic systems is very complicated since there are five viscosities involved [11], and four of these viscosities diverge as ω^{-1} in the low-frequency limit [12]. These divergences are the direct consequence of the anharmonic terms in the elastic energy of the smectic-*A* phase, which are required by the rotational invariance of the free energy [13]. However, the wave-vector and frequency regimes that dominate the layer displacement fluctuations—which prove to be the regime $\omega \sim q_z \sim q_\perp^2$, where q_z and q_\perp denote the wavevector components parallel and perpendicular to the layer normal, respectively—are unaffected by the nonlinearities [12], except for the weak logarithmic Grinstein-Pelcovits effects on the statics [13].

In our previous paper [14], we formulated the hydrodynamic description of smectic-*A* films. Our work was a direct generalization of the hydrodynamics for bulk smectic-*A* systems to the so called “sliding geometry” [15]. We derived expressions for the time-dependent displacement and density autocorrelation functions for smectic-*A* systems both in the thermodynamic limit, and in the finite size, nonzero surface tension limit, which applies to real freely suspended smectic-*A* films. To do this, we used the linearized hydrodynamic equations for the smectic-*A* phase, and the Gaussian model of the layer fluctuations. If permeation is neglected, the smectic layers move at the same rate as the local fluid does, and then the hydrodynamics of bulk smectic-*A* liquid crystals in the sliding geometry can be described by only one variable, namely the local displacement field $u(\mathbf{r}, t)$. This assumption is supported by a recent study by Chen and Jasnow [16] on the dynamics of smectic-*A* films. They show that the permeation constant does not affect the power law spectral behavior of the surface fluctuations.

Then in the Fourier representation, we found the following equation of motion:

$$\rho_0 \frac{\partial^2 u(\mathbf{q}, t)}{\partial t^2} = -\eta_3 q_\perp^2 \frac{\partial u(\mathbf{q}, t)}{\partial t} - (Bq_z^2 + Kq_\perp^4) u(\mathbf{q}, t). \quad (1.1)$$

Here ρ_0 is the average mass density, η_3 is the layer sliding viscosity, and K and B are the elastic constants corresponding to the layer bend and compression, respectively. The

physical sense of this equation is simple: it expresses Newton’s second law for the acceleration along the z direction in terms of the elastic and viscous forces. Eq. (1.1) results from the complete set of hydrodynamic equations [15] when it is assumed that the density adjusts to the layer distortions, i.e., the isotropic part of the stress tensor vanishes, and when the wave vector is in the regime $q_z \ll q_\perp$ (the sliding geometry), which is the regime of interest in the calculation of the displacement autocorrelation function. This is because for typical thermotropic smectic-*A* materials $(K/B)^{1/2}$ is of order of the layer spacing, which means that the wavelengths of the thermally excited compression modes are much longer than the wavelengths of the thermally excited undulation modes. This allows us to greatly simplify the hydrodynamics for the smectic-*A* phase.

It is well known that in the general case when \mathbf{q} is oblique with respect to the layers there are two pairs of propagating modes, referred to as the “first sound” and the “second sound,” respectively [17]. These acoustic waves satisfy hydrodynamic equations in the limit of small wavevectors (no dissipation). Quite often these modes decouple, i.e., the first is essentially a density modulation, whereas the second corresponds to a modulation of u . Then the speed of the first sound c_1 is isotropic as in ordinary fluids. The speed of the second sound, however, is strongly anisotropic, and it is given by $c_2 \approx (B/\rho_0)^{1/2} \sin \theta \cos \theta$, where θ is the angle between \mathbf{q} and the optical axis. This decoupling occurs in the limit of an incompressible fluid. It is also satisfied when $q_z \ll q_\perp$. It can also be shown that in both limits the contribution of the first sound to the dynamic displacement autocorrelation function is negligible. This means that we have to consider only the second sound mode, which becomes damped when the viscosity is switched on. Note that this mode is correctly described by Eq. (1.1) for θ close to $\pi/2$. Indeed, neglecting the terms of higher order than q^2 we find the dispersion relation: $\omega = (B/\rho_0)^{1/2} q_z$, which corresponds to the second sound when $q_z \ll q_\perp$.

In Ref. [14], we assumed that the inertial term is negligible, which means that the smectic-*A* hydrodynamics could be studied in terms of the overdamped limit. This approximation is self-consistent provided that

$$\epsilon = \frac{\rho_0 K}{\eta_3^2} \ll 1. \quad (1.2)$$

For a typical smectic-*A* liquid crystal we find $\epsilon \sim 10^{-6} - 10^{-5}$, thus, in the wave-vector regime: $Bq_z^2 \sim Kq_\perp^4$, the inertial term can indeed be neglected. Then the relaxation time τ_q of the \mathbf{q} mode is given by [15]

$$\tau_q = \frac{\eta_3 q_\perp^2}{Bq_z^2 + Kq_\perp^4}. \quad (1.3)$$

Thus, the relaxation time τ_q diverges as $q_\perp \rightarrow 0$, provided that $Bq_z^2 \sim Kq_\perp^4$. This divergence is a direct consequence of the slow Goldstone mode associated with the broken translational symmetry.

It is possible to obtain an explicit expression for the dynamic density autocorrelation function $G(\mathbf{r}, t)$ in the thermo-

dynamic limit, albeit in terms of special functions. The scaling form of $G(\mathbf{r}, t)$ is given by [14]

$$G(\mathbf{r}, t) = \left(\frac{r_{\perp}}{a_0}\right)^{-2\eta} h\left(\frac{2\sqrt{KB}t}{\eta_3|z|}, \frac{r_{\perp}^2}{4\lambda|z|}\right), \quad (1.4)$$

where $\eta = q_z^2 k_B T / (8\pi\sqrt{KB})$ is the static exponent [1], $\lambda = \sqrt{K/B}$, a_0 denotes the molecular size cutoff, and $h(\phi, \psi)$ is the scaling function. The three asymptotic behaviors of $G(\mathbf{r}, t)$ (which occur in the two different large distance limits, and the long time limit), are given by

$$G(r_{\perp}, z, t) \sim \begin{cases} (4\lambda|z|/a_0^2)^{-\eta} & \text{for } |z| \rightarrow \infty \\ (16Kt/\eta_3 a_0^2)^{-\eta} & \text{for } t \rightarrow \infty \\ (r_{\perp}/a_0)^{-2\eta} & \text{for } r_{\perp} \rightarrow \infty. \end{cases} \quad (1.5)$$

Here $|z|$ is the distance parallel to the layer normal, r_{\perp} is the distance perpendicular, and t is the time.

To study finite-size smectic-A films, we used the discrete model [14]. In this model, the deformations of the film are described by a set of functions $u_n(\mathbf{r}_{\perp}, t)$ ($n=0, \dots, N$), where $N+1=L$ is the number of smectic layers in the film. Thus, Ld is the thickness of the film (d is the layer spacing). This discrete model was developed earlier to describe the static correlation functions [5]. Any arbitrary deformation can be expressed in terms of the L normal modes, which, in the Fourier representation, are functions of \mathbf{q}_{\perp} . Consequently, the decay of the deformation is described by L relaxation times $\tau^{(k)}(q_{\perp})$ ($k=0, \dots, N$). We studied the finite-size problem using the same overdamped approximation as in the bulk case. Then the longest relaxation time, corresponding to the $k=0$ mode, has a finite value in the limit obtained for $q_{\perp} \rightarrow 0$, which is given by

$$\tau_0 = \tau^{(0)}(q_{\perp}=0) = Ld \frac{\eta_3}{2\gamma}. \quad (1.6)$$

Here γ is the surface tension. This predicted form of the scaling of τ_0 with the film thickness has been confirmed in a recent coherent soft x-ray dynamic light scattering (SXDLs) experiment [14,18]. The experimentally measured ratio of $\eta_3/2\gamma$ determined using SXDLs is in good agreement with independent measurements of η_3 and γ separately [19–21]. In our previous paper [14], we showed that the overdamping assumed in our theoretical analysis is self-consistent for $q_{\perp} \gg q_c$; the value of q_c is given by

$$q_c = \sqrt{\frac{2\rho_0\gamma}{\eta_3^2 dL}}. \quad (1.7)$$

For typical values of the smectic-A parameters, we find

$$q_c \sim \sqrt{\frac{2}{L}} \times 10^4 \text{ cm}^{-1}. \quad (1.8)$$

This means that the length scale defined by q_c is comparable to our experimental resolution cutoff Λ . Note, however, that for $q_{\perp} \leq q_c$, the inertial term cannot be neglected.

The asymptotic behavior of G in the finite-size case is different from the bulk case. Previously, we studied [14]

only the asymptotics for $r_{\perp} \rightarrow \infty$. We found an algebraic decay with the time-dependent exponent

$$x(t) = \frac{k_B T q_z^2}{4\pi\gamma} \exp\left(-\frac{t}{\tau_0}\right). \quad (1.9)$$

This result is consistent with the overdamped limit for $a_0 \ll r_{\perp} \ll q_c^{-1}$.

In this paper, we study the dynamic density autocorrelation function for a finite-size, nonzero surface tension smectic-A film in more detail. We concentrate on the scaling properties of $G(\mathbf{r}, t)$. In order to obtain the complete picture, we do not neglect the inertial term in the linearized hydrodynamic equations, as this term becomes important in the $q_{\perp} \rightarrow 0$ limit. We expect that our predictions concerning the time-dependent exponent for the range of r_{\perp} specified above will not be changed. However, they will be modified for $r_{\perp} \gg q_c^{-1}$. It is interesting to see how the crossover between different asymptotic regimes occurs. We also investigate the crossover between the bulk and the finite-size smectic-A film behavior, and the scaling of the dynamic density autocorrelation function with the film thickness.

When the system is finite in the z direction, the density autocorrelation function (which is defined precisely in Sec. II) also depends on the film thickness. In this paper, we propose the following scaling form for the density autocorrelation function,

$$G(r_{\perp}, l, t; L) = L^{-\eta f} \left(\frac{r_{\perp}}{\sqrt{\lambda d L}}, \frac{|l|}{L}, \frac{t}{\tau_0} \right). \quad (1.10)$$

Here the integer variable l denotes the difference between the layer indices. We will show that this scaling form is well satisfied, except for very thin films where small deviations occur. For thick films, we find that $G(\mathbf{r}, t)$ has a region of a bulklike behavior as predicted by formula (1.4).

The rest of this paper is organized as follows. In Sec. II, we define the discrete model and calculate the formal expressions for the displacement and the density autocorrelation functions. In Sec. III, we compare the predictions of the scaling form (1.10) with the results of numerical calculations, to determine the range of validity of the scaling form. Finally, in Sec. IV, we discuss our results and present our conclusions.

II. THE DISCRETE MODEL FOR FINITE-SIZE SMECTIC-A FILMS

A detailed treatment of the dynamics of a discrete stack of membranes representing lyotropic smectic liquid crystals has been presented by Ramaswamy *et al.* [22]. Here we consider a generalization of Eq. (1.1) to the case of finite-size smectic-A films. This generalization is rather straightforward. The discrete version of the harmonic Hamiltonian is given by [5]

$$H = \frac{1}{2} \int d^2 r_{\perp} \left\{ dB \sum_{n=0}^{N-1} \left(\frac{u_{n+1} - u_n}{d} \right)^2 + dK \sum_{n=1}^{N-1} (\Delta_{\perp} u_n)^2 + \gamma [(\nabla_{\perp} u_0)^2 + (\nabla_{\perp} u_N)^2] + K_s [(\Delta_{\perp} u_0)^2 + (\Delta_{\perp} u_N)^2] \right\}. \quad (2.1)$$

Here $u_n(\mathbf{r}_\perp, t)$ denotes the deviation of the n th layer from its equilibrium position. The surface layer bend elastic constant K_s (which has dimensions of dyn cm) acts only at the two surface layers ($n=0$ and $n=N$). Because of missing neighbors K_s can differ from Kd . We assume that the system is translationally invariant in the xy plane. Thus, in the Fourier representation, the hydrodynamic equation [14,23] has a form of L coupled second-order differential equations for $u_n(\mathbf{q}_\perp, t)$, i.e.,

$$\left(\rho_0 \frac{\partial^2}{\partial t^2} + \eta_3 q_\perp^2 \frac{\partial}{\partial t} + \frac{K_s q_\perp^4 + \gamma q_\perp^2}{d} \right) u_0 = B \frac{u_1 - u_0}{d^2}, \quad (2.2a)$$

$$\left(\rho_0 \frac{\partial^2}{\partial t^2} + \eta_3 q_\perp^2 \frac{\partial}{\partial t} + K q_\perp^4 \right) u_n = B \frac{u_{n+1} - 2u_n + u_{n-1}}{d^2} \quad \text{for } n=1, \dots, N-1, \quad (2.2b)$$

$$\left(\rho_0 \frac{\partial^2}{\partial t^2} + \eta_3 q_\perp^2 \frac{\partial}{\partial t} + \frac{K_s q_\perp^4 + \gamma q_\perp^2}{d} \right) u_N = B \frac{u_{N-1} - u_N}{d^2}. \quad (2.2c)$$

It is convenient to introduce the following dimensionless variables: $\mathbf{Q} = \sqrt{\lambda d} \mathbf{q}_\perp$, $\mathbf{R} = \mathbf{r}_\perp / \sqrt{\lambda d}$, and $t \rightarrow t \eta_3 d / \sqrt{KB}$, where $\eta_3 d / \sqrt{KB}$ has the dimension of time. For simplicity, we use the same symbol for the dimensionless time. Now, it is convenient to introduce matrix notation, in which the Hamiltonian and the equation of motion can be expressed in the following compact form

$$H = \frac{B}{2d} \sum_{\mathbf{Q}} u^\dagger(\mathbf{Q}) M(\mathbf{Q}) u(\mathbf{Q}), \quad (2.3)$$

where u is the $L \times 1$ matrix with components $u_n(n=0, \dots, N)$, u^\dagger is the matrix adjoint to u , and

$$\left[\epsilon \frac{\partial^2}{\partial t^2} + Q^2 \frac{\partial}{\partial t} + M(\mathbf{Q}) \right] u(\mathbf{Q}, t) = 0. \quad (2.4)$$

Here $M(\mathbf{Q})$ is an $L \times L$ tridiagonal symmetric matrix defined by

$$M_{00} = M_{NN} = 1 + \bar{\gamma} Q^2 + \bar{K}_s Q^4, \quad (2.5a)$$

$$M_{nn} = 2 + Q^4, \quad \text{for } n=1, \dots, N-1, \quad (2.5b)$$

$$M_{n(n-1)} = M_{n(n+1)} = -1, \quad \text{for } n=1, \dots, N-1. \quad (2.5c)$$

Here we have introduced two dimensionless parameters: $\bar{\gamma} = \gamma / \sqrt{KB}$ and $\bar{K}_s = K_s / Kd$.

A. Displacement-displacement correlation function

In the discrete model, we can treat the displacement-displacement correlation function as an $L \times L$ symmetric matrix $C(\mathbf{Q}, t)$ with the components given by

$$C_{nm}(\mathbf{Q}, t) = \langle u_n(\mathbf{Q}, t) u_m(-\mathbf{Q}, 0) \rangle, \quad (2.6)$$

where $\langle \dots \rangle$ denotes the equilibrium average over all displacements at $t=0$, with the weight proportional to the Boltzmann factor $\exp(-H/k_B T)$. The equation of motion for $C(\mathbf{Q}, t)$ follows from Eq. (2.4) when both sides of (2.4) are multiplied by $u(-\mathbf{Q}, 0)$ and the thermal average is taken. This procedure gives

$$\left[\epsilon \frac{\partial^2}{\partial t^2} + Q^2 \frac{\partial}{\partial t} + M(\mathbf{Q}) \right] C(\mathbf{Q}, t) = 0. \quad (2.7)$$

The formal solution of this equation for $t \geq 0$ is given by

$$\begin{aligned} C(\mathbf{Q}, t) &= C(\mathbf{Q}, 0) \\ &\times [\alpha_+(\mathbf{Q}) - \alpha_-(\mathbf{Q})]^{-1} \{ \alpha_+(\mathbf{Q}) \exp[\alpha_-(\mathbf{Q})t] \\ &- \alpha_-(\mathbf{Q}) \exp[\alpha_+(\mathbf{Q})t] \}, \end{aligned} \quad (2.8)$$

where the matrices $\alpha_\pm(\mathbf{Q})$ satisfy the quadratic equation

$$\epsilon \alpha_\pm^2(\mathbf{Q}) + Q^2 \alpha_\pm(\mathbf{Q}) + M(\mathbf{Q}) = 0. \quad (2.9)$$

The initial conditions at $t=0$

$$C(\mathbf{Q}, 0) = \frac{k_B T d}{B} M^{-1}(\mathbf{Q}), \quad (2.10a)$$

and

$$\left[\frac{\partial C(\mathbf{Q}, t)}{\partial t} \right]_{t=0} = 0 \quad (2.10b)$$

must be satisfied. The second equation follows from the fact that $u(\mathbf{Q}, 0)$ and $\partial_t u(\mathbf{Q}, 0)$ are statistically independent.

The spatiotemporal Fourier transform of the displacement autocorrelation function is given by

$$\begin{aligned} C(\mathbf{Q}, \omega) &= \int_{-\infty}^{+\infty} dt \exp(-i\omega t) C(\mathbf{Q}, t) \\ &= \frac{2dk_B T}{B\omega} \text{Im} [M(\mathbf{Q}) - (\epsilon\omega^2 + i\omega Q^2)I]^{-1} \end{aligned} \quad (2.11)$$

where I denotes the unit matrix, and we have used the time-reversal symmetry of $C(\mathbf{Q}, t)$. In the previous paper (see Appendix B in [14]) we presented a method for obtaining an explicit expression for $M^{-1}(\mathbf{Q})$. Using the same method it is also possible to give an explicit formula for the inverse matrix in Eq. (2.11). This might be of some use in analytical studies of the asymptotic behavior of the displacement autocorrelation function in real space. However, since we study the problem numerically, we do not take this route.

In an alternative approach, used in this paper, $M(\mathbf{Q})$ is diagonalized (see Appendix B in [14]) and $C(\mathbf{Q}, t)$, which is a matrix function of $M(\mathbf{Q})$, is also expressed in this diagonal representation. The k th eigenvalue of $\alpha_\pm(\mathbf{Q})$ ($k=0, \dots, N$) can be expressed in terms of the k th eigenvalue of $M(\mathbf{Q})$, $\lambda^{(k)}(\mathbf{Q})$, via the relaxation time $\tau_\pm^{(k)}(\mathbf{Q})$ and the frequency $\omega^{(k)}(\mathbf{Q})$ of the k th mode as follows:

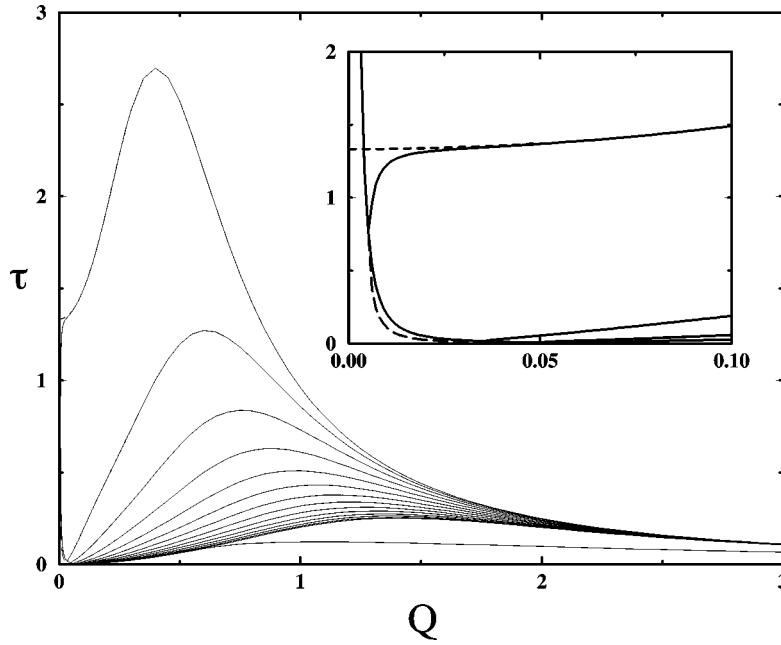


FIG. 1. Relaxation times [in units of $\eta_3 d / (KB)^{1/2}$] of normal modes vs Q for a 16 layer thick film with the parameters $\epsilon = 10^{-5}$, $\bar{\gamma} = 6$, $\bar{K}_s = 1$. The inset shows the region of small wave vectors. In the main panel, $\tau_{\pm}^{(k)}$ is plotted as the solid line. In the inset, $\tau^{(0)}$ (which has been obtained from the overdamped limit where $\epsilon = 0$) is plotted as the dashed line. Note that in this inset plot, only the branch $\tau_{-}^{(0)}$ —which is represented by the long dashed line—can be seen.

$$\alpha_{\pm}^{(k)}(Q) = -\frac{1}{\tau_{\pm}^{(k)}(Q)} \pm i\omega^{(k)}(Q), \quad (2.12)$$

where

$$\omega^{(k)}(Q) = 0, \quad (2.13a)$$

$$\tau_{\pm}^{(k)}(Q) = \frac{2\epsilon}{Q^2 \mp \sqrt{Q^4 - 4\epsilon\lambda^{(k)}(Q)}}, \quad (2.13b)$$

if $Q^4 > 4\epsilon\lambda^{(k)}(Q)$ and

$$\tau_{\pm}^{(k)}(Q) = \frac{2\epsilon}{Q^2}, \quad (2.14a)$$

$$\omega^{(k)}(Q) = \frac{1}{2\epsilon} \sqrt{|Q^4 - 4\epsilon\lambda^{(k)}(Q)|}, \quad (2.14b)$$

otherwise. All relaxation times eventually diverge in the limit $Q \rightarrow 0$. However, because $\epsilon \sim 10^{-6} - 10^{-5}$ is very small, this divergence can only be seen for rather small wave vectors. The frequencies of the $k \neq 0$ modes have finite limits when $Q \rightarrow 0$. For the $k = 0$ mode, and for small wave vectors, it can be shown [14] that

$$\lambda^{(0)}(Q) \approx \frac{2\bar{\gamma}Q^2}{L}. \quad (2.15)$$

Hence, $\omega^{(0)}(Q) \rightarrow 0$ when $Q \rightarrow 0$. In Fig. 1, we plot the relaxation times vs Q , and the small wave-vector regime is shown in the inset. The cusps correspond to the change of

branch [see Eqs. (2.13) and (2.14)]. For comparison, we also show $\tau^{(0)}$ obtained from the overdamped limit ($\epsilon = 0$); it has a finite limit for $Q \rightarrow 0$.

B. Density-density correlation function

We start with the center-of-mass density operator [5]

$$\hat{\rho}(\mathbf{r}_{\perp}, t) = \rho_s \sum_{n=0}^N \delta(z - nd - u_n(\mathbf{r}_{\perp}, t)), \quad (2.16)$$

where ρ_s is the density of molecules in the smectic layer. The corresponding density-density correlation function in the Fourier representation is defined to be

$$\begin{aligned} \langle \hat{\rho}(\mathbf{q}, t) \hat{\rho}(-\mathbf{q}, 0) \rangle &= \rho_s^2 \mathcal{A} \int d^2 r_{\perp} \exp(i\mathbf{q}_{\perp} \cdot \mathbf{r}_{\perp}) \\ &\times \sum_{n,m=0}^N \exp[i(n-m)dq_z] \mathcal{G}(r_{\perp}, n, m, t), \end{aligned} \quad (2.17)$$

where \mathcal{A} is the area of the film, and where

$$\begin{aligned} \mathcal{G}(r_{\perp}, n, m, t) &= \langle \exp[iq_z [u_n(\mathbf{r}_{\perp}, t) - u_m(\mathbf{0}, 0)]] \rangle \\ &= \exp[-\frac{1}{2} q_z^2 g_{nm}(r_{\perp}, t)] \end{aligned} \quad (2.18)$$

with

$$g_{nm}(r_{\perp}, t) = \langle [u_n(\mathbf{r}_{\perp}, t) - u_m(\mathbf{0}, 0)]^2 \rangle.$$

In Eq. (2.18) we have used the fact that u is a Gaussian random variable. In terms of dimensionless variables, we obtain

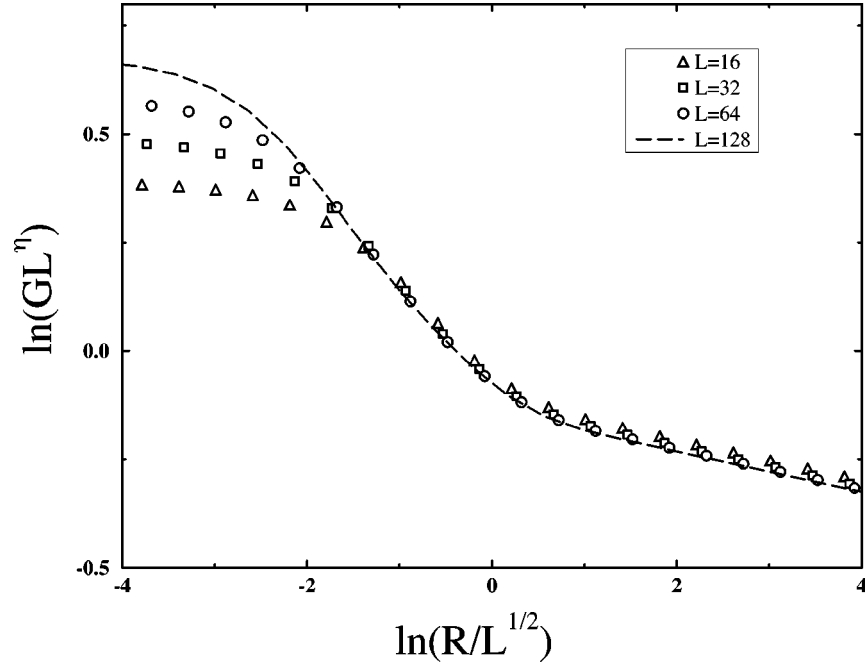


FIG. 2. $\ln(GL^\eta)$ as a function of $\ln(R/L^{1/2})$, for $l=0$ and $t=0$. In this figure, we display the results for the film thicknesses $L=16, 32, 64$, and 128 .

$$g_{nm}(R, t) = \frac{k_B T}{2\pi\sqrt{KB}} \int_0^\infty Q dQ [\bar{C}_{nn}(Q, 0) + \bar{C}_{mm}(Q, 0) - 2J_0(QR)\bar{C}_{nm}(Q, t)] \quad (2.19)$$

Here J_0 denotes the zeroth-order Bessel function, and $\bar{C} = (B/dk_B T)C$ is dimensionless ($\bar{C} = M^{-1}$ at $t=0$). In the same overdamped limit approximation used in Ref. [14], this integral has a logarithmic divergence at $Q=0$. Thus, it was necessary to introduce a cutoff at small wave vectors. This problem does not appear here, since all of the relaxation times diverge when $Q \rightarrow 0$, and the integrand remains finite at $Q=0$.

Transforming the double sum in Eq. (2.17), we obtain

$$\begin{aligned} & \langle \hat{\rho}(\mathbf{q}, t) \hat{\rho}(-\mathbf{q}, 0) \rangle \\ &= \rho_s^2 \mathcal{A} L \int d^2 r_\perp \exp(i\mathbf{q}_\perp \cdot \mathbf{r}_\perp) \sum_{l=-N}^N \exp(ildq_z) G(r_\perp, l, t), \end{aligned} \quad (2.20)$$

where, by definition,

$$G(r_\perp, l, t) = \frac{1}{L} \sum_{n=0}^{N-|l|} \mathcal{G}(r_\perp, n, n+|l|, t). \quad (2.21)$$

Thus, G is a function only of the layer indices difference, whereas \mathcal{G} is a function of both indices. This is similar to bulk smectic- A systems. If the limit $N \rightarrow \infty$ is taken at constant l , then G reduces to \mathcal{G} . For simplicity, the dependence of \mathcal{G} and G on q_z and the film thickness has been suppressed. In the next section we study the dependence of G on the four variables: r_\perp, l, t , and L , for a wave vector satisfying the Bragg condition, i.e., for $q_z = 2\pi/d$.

III. SCALING FORM OF THE CORRELATION FUNCTION G FOR SMECTIC- A FILMS

In this section, we present the results of our numerical studies of the density autocorrelation function $G(r_\perp, l, t; L)$. Our goal was to check whether the scaling form of G presented in Sec. I [see Eq. (1.10)] is correct. We have performed numerical calculations of G for the following set of dimensionless parameters: $\bar{\gamma} = 6, \epsilon = 10^{-5}, \bar{K}_s = 1, k_B T / (d^2 \sqrt{KB}) = 4/45$, and $q_z d = 2\pi$. For practical reasons, we have also introduced a cutoff at large wavevectors, Q_{\max} , to calculate the integral in Eq. (2.19), although this integral has a finite limit when $Q_{\max} \rightarrow \infty$. In our calculations, we used $Q_{\max} = 40$. This set of parameters corresponds roughly to typical experimental values: $k_B T = 4 \times 10^{-14}$ erg, $K = 10^{-6}$ dyn, $B = 2.5 \times 10^7$ dyn/cm², $d = 30$ Å, $\gamma = 30$ dyn/cm, $\rho_0 = 1$ g/cm³, $\eta_3 = 0.3$ g/(cm s), and $a_0 = 4$ Å.

First, we studied GL^η as a function of one of the scaled variables when the remaining two variables are set to zero, to check whether the bulk asymptotic behavior is recovered when $L \rightarrow \infty$. In other words, the scaling function $f(\phi, \psi, v)$ must have the following properties:

$$f(\phi, 0, 0) \sim \phi^{-2\eta} \quad \text{for } \phi \rightarrow 0, \quad (3.1)$$

$$f(0, \psi, 0) \sim \psi^{-\eta} \quad \text{for } \psi \rightarrow 0, \quad (3.2)$$

$$f(0, 0, v) \sim v^{-\eta} \quad \text{for } v \rightarrow 0. \quad (3.3)$$

In Fig. 2, we plot $\ln(GL^\eta)$ vs $\ln(R/L^{1/2})$ for a few values of L . The scaling relation is rather well satisfied for $R \gg 1$ and for thick films. For thin films larger deviations occur. In the region of very small R , i.e. $R \sim 1$ or smaller, the scaling does not hold at all, and the limit $R \rightarrow 0$ depends on L . In the region where the scaling is approximately satisfied, we can

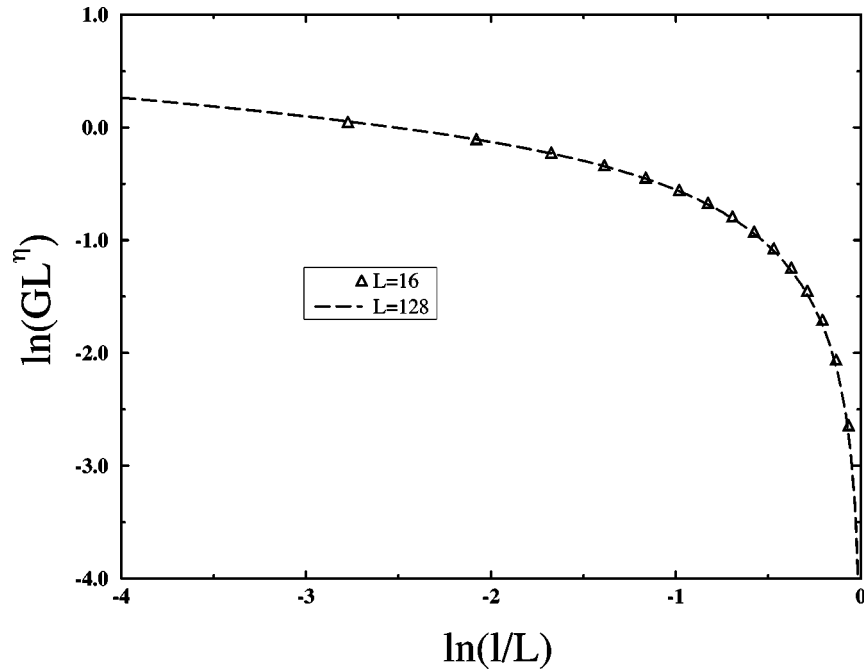


FIG. 3. $\ln(GL^\eta)$ as a function of $\ln(l/L)$, for $R=0$ and $t=0$. In this figure, we display the results for the film thicknesses $L=16$ and 128 .

distinguish two asymptotic regimes: (1) $R \ll L^{1/2}$ and (2) $R \gg L^{1/2}$. In the first regime, the slope of the ‘linear’ part is $\approx -2\eta$, in agreement with Eq. (3.1). In the second regime, the slope approaches $-\chi$, where $\chi = k_B T q_z^2 / (4\pi\gamma)$.

In Fig. 3, $\ln(GL^\eta)$ as a function of $\ln(l/L)$ is shown, for $L=16$ and 128 . The two curves are practically indistinguishable from each other. Some deviations from the scaling occur only for extremely thin films ($L=4$). Here only one asymptotic regime, for $l \ll L$ can be observed. The slope of the curve approaches $-\eta$ when $l/L \rightarrow 0$, in agreement with Eq. (3.2).

The plot $\ln(GL^\eta)$ vs $\ln(t/\tau_0)$ is presented in Fig. 4. It is very similar to the plot shown in Fig. 2. Large deviations from the scaling relation occur for very short times. Then there is a region of a quasibulk behavior for $t \ll \tau_0$, i.e., the slope of the curves is close to $-\eta$ [see Eq. (3.3)], and finally, the slope approaches $-\chi$ when $t \gg \tau_0$. The scaling becomes more accurate for thick films, whereas for thin films larger deviations occur.

In Figs. 5 and 6, we present $\ln(GL^\eta)$ as a function of $\ln(R/L^{1/2})$ at $t=0$ and $\ln(GL^\eta)$ as a function of $\ln(t/\tau_0)$ at $R=0$, respectively, for a few values of the ratio L/l and for a

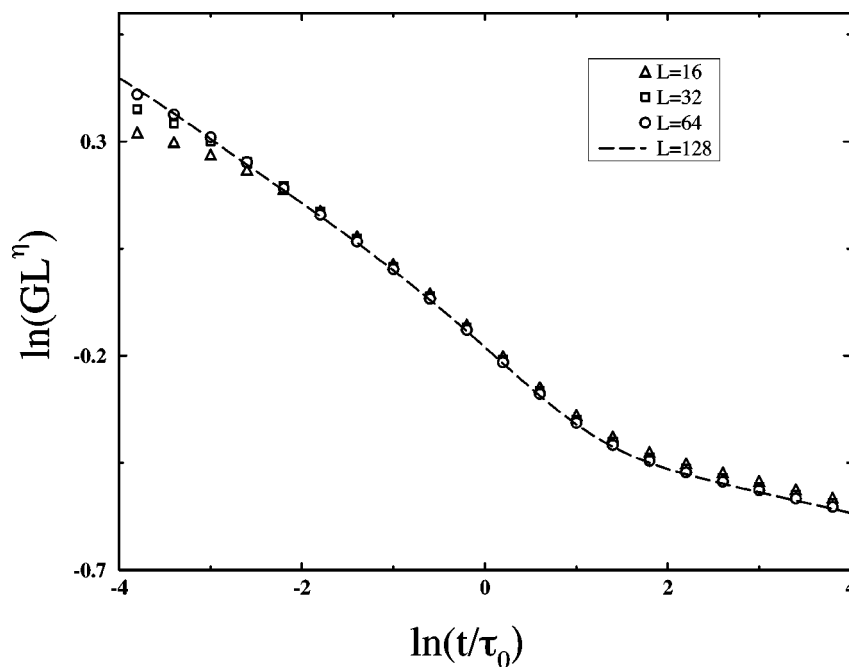


FIG. 4. $\ln(GL^\eta)$ as a function of $\ln(t/\tau_0)$, for $R=0$ and $l=0$. In this figure, we display the results for the film thicknesses $L=16, 32, 64$, and 128 .

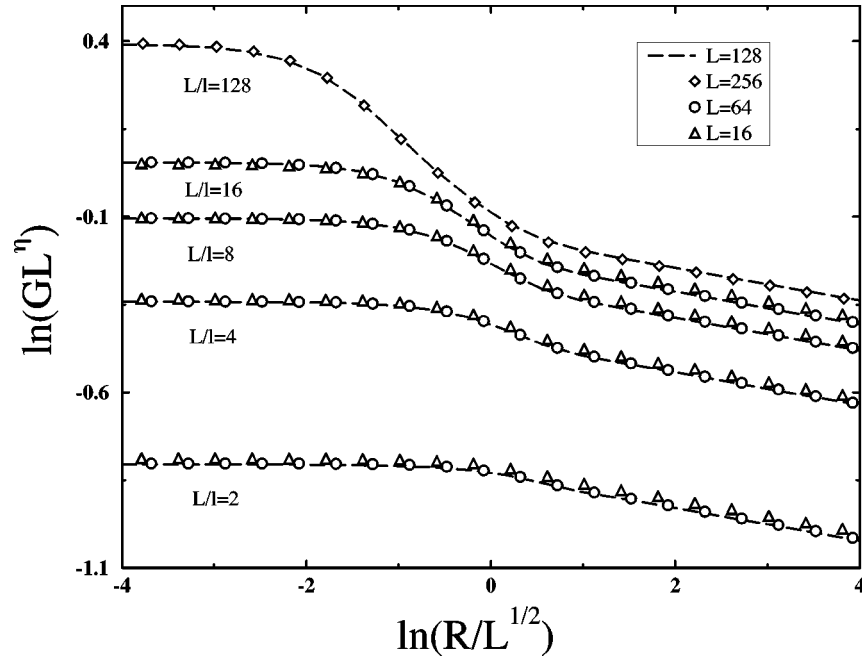


FIG. 5. $\ln(GL^\eta)$ in the static case ($t=0$) as a function of $\ln(R/L^{1/2})$. In this figure, a few values of the ratio L/l are shown for the thicknesses $L = 16, 64, 128$, and 256 . Starting from the top, we display the curves for the ratio values $L/l = 128, 16, 8, 4$, and 2 .

few values of L . In order to study the scaling form of G , we have chosen a particular set of l , for which the ratio L/l is an integer. In this way we can easily compare the results for different L . It is clear from these plots that when $l \neq 0$ the scaling is very well satisfied even in the region of very small R or t .

The dependence of $\ln(GL^\eta)$ on $\ln(t/\tau_0)$ for a few values of the ratio $R/L^{1/2}$ and $l=0$ is shown in Fig. 7. For $t \gg \tau_0$ the slope of all curves approaches $-\chi$.

In Fig. 8, we plot $\ln(GL^\eta)$ vs $\ln(R/L^{1/2})$ for a few ratios t/τ_0 and L/l . All curves approach the same slope ($-\chi$) in

the limit $R/L^{1/2} \rightarrow \infty$. For $R > L^{1/2}$ there exists an intermediate region of approximately linear dependence with a time dependent slope. This is shown in Fig. 9, where the derivative $d(\ln G)/d(\ln R)$ is plotted against t/τ_0 , at $\ln(R/L^{1/2}) = 2$. This is in a very good agreement with the asymptotic behavior of G for large R , i.e., with $G \sim R^{-x(t)}$ as predicted in Ref. [14].

IV. DISCUSSION

We have proposed a simple scaling form for the dynamic density autocorrelation function $G(\mathbf{r}, t)$ for smectic-A films.

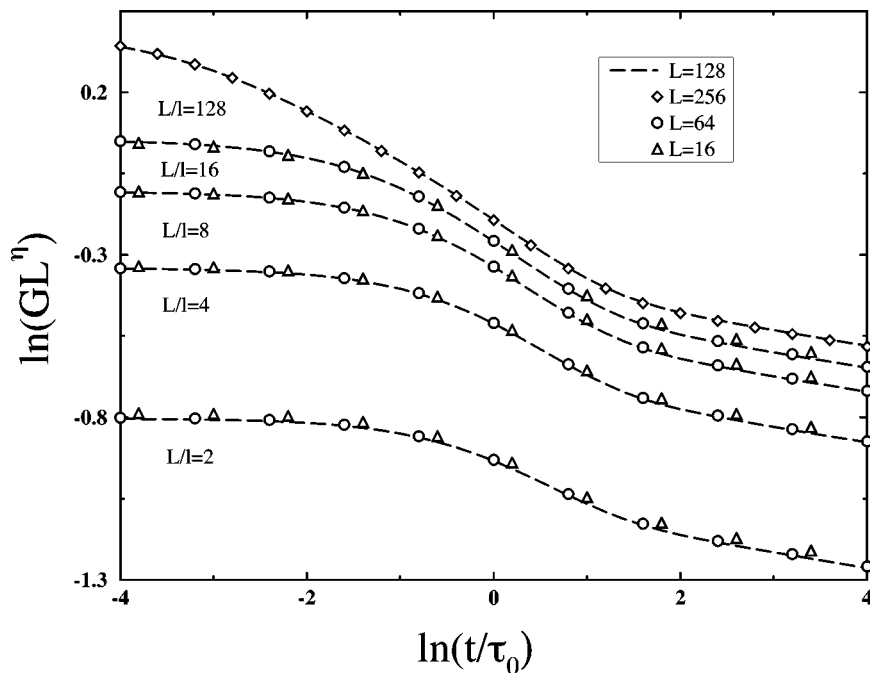


FIG. 6. $\ln(GL^\eta)$ as a function of the dimensionless time variable $\ln(t/\tau_0)$ for $R=0$. The choices of the values of the ratios L/l and of the thicknesses L are the same as in Fig. 5.

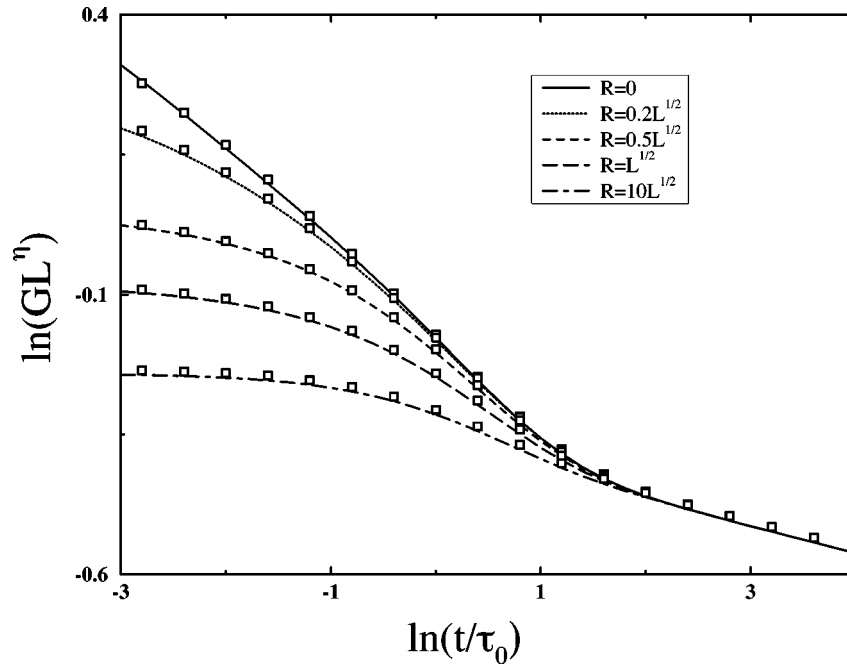


FIG. 7. $\ln(GL^\eta)$ as a function of the dimensionless time $\ln(t/\tau_0)$. In this figure, $l=0$, and $R/L^{1/2}=0,0.2,0.5,1$, and 10 . The lines and the squares correspond to the thickness values $L=64$ and $L=32$, respectively.

Our work is based on (1) linearized hydrodynamics, and (2) the Gaussian model of thermally driven layer fluctuations in the smectic- A phase. We tested our postulated scaling form by detailed, real-space numerical calculations of $G(\mathbf{r},t)$. Since G depends on four variables—the two distances z and r_\perp , the time t , and the film thickness Ld —it is rather difficult to completely verify the postulated scaling form numerically. Consequently, we have not attempted very detailed systematic studies of the dependence of G on the extra con-

trol parameters provided by the bulk and surface smectic- A material parameters—namely: K , B , η_3 , γ , and K_s . Nevertheless, the results that we obtained using typical values of these parameters strongly suggest that the postulated scaling form works very well, except for very thin films. In the limit of infinitely thick films, we recover the asymptotic form that we obtained previously—by neglecting inertia—for the smectic- A phase in the thermodynamic limit [14]. It is interesting that the inclusion of the inertial term in the hydrody-

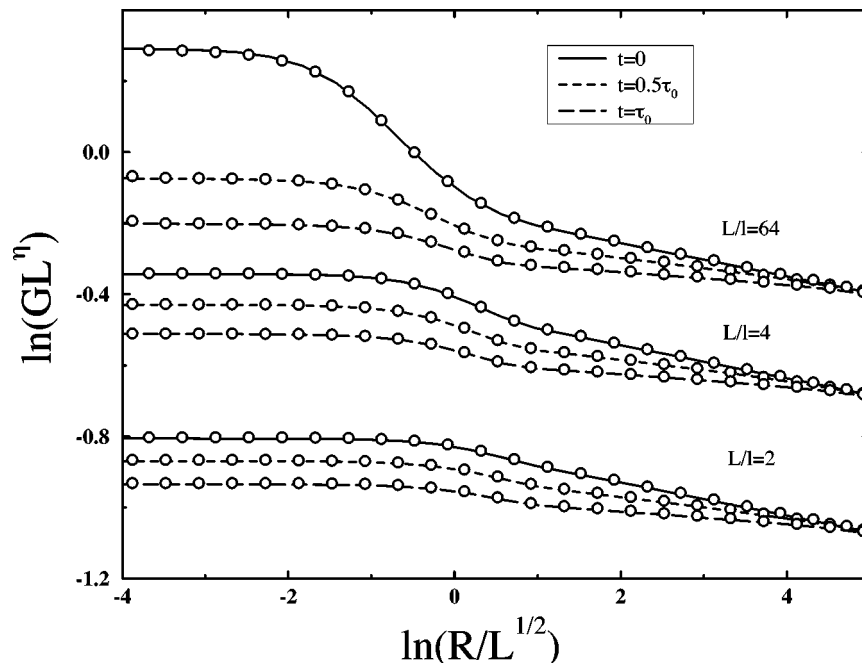


FIG. 8. $\ln(GL^\eta)$ as a function of $\ln(R/L^{1/2})$ for the dimensionless time values $t/\tau_0=0,0.5$, and 1 . In this figure, three values of the ratio L/l are shown; starting from the top, we display $L/l=64,4$, and 2 . The lines and the circles correspond to the thickness values $L=128$ and $L=64$, respectively.

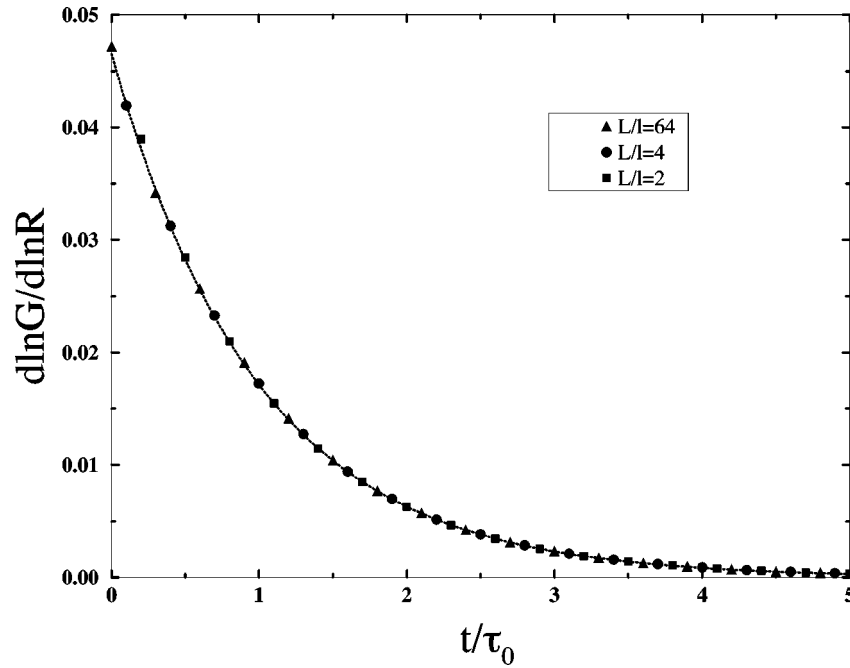


FIG. 9. The logarithmic slope $d \ln G / d \ln R$ with $\ln(R/L^{1/2})=2$ (see Fig. 8) as a function of t/τ_0 . In this figure, the logarithmic slope vs dimensionless time plots are shown for the ratios $L/l=64, 4$, and 2 when the thickness $L=64$. The dashed line corresponds to the exponent $x(t)$ defined by Eq. (1.9).

dynamic equation of motion leads to the scaling form of G in which the time scale is given by the relaxation time τ_0 obtained from the overdamped, no inertia, approximation. However, the divergence of the true relaxation times, in the small perpendicular wave-vector $q_\perp \rightarrow 0$ limit, manifests itself in the long distance behavior of the dynamic correlation function, which approaches the static correlation function in the limit $r_\perp \rightarrow \infty$. Thus, the long distance behavior of $G(\mathbf{r}, t)$ in the direction parallel to the film is characterized by an algebraic decay with the surface exponent χ . The long time behavior for films also differs from the predictions for bulk smectic- A liquid crystals. We observe that for times $t \sim 10\tau_0$ or longer G also decays algebraically with the surface exponent χ .

We have also verified that the sum of $G(r_\perp, l, t)$ over l at $q_z = 2\pi/d$ [see Eq. (2.20)] scales with the thickness of the film as $L^{1-\eta}$, provided that the film is sufficiently thick ($L \sim 100$). This shows that the sum is well approximated by the integral over l/L . In this approximation, we obtain the following scaling form of the dynamic structure factor

$$S(\mathbf{q}, t) \propto L^{1-\eta} q_\perp^{-2} F(q_\perp \sqrt{\lambda d L}, t/\tau_0), \quad (4.1)$$

where

$$F(\phi, \nu) = \int_0^\infty s ds J_0(s) L^{-1} \sum_{l=-N}^N f(s/\phi, |l|/L, \nu).$$

In the limit as $q_\perp \rightarrow 0$, we find

$$S(\mathbf{q}, t) \sim L^{1-\eta+\chi/2} q_\perp^{-2+\chi}. \quad (4.2)$$

However, since the decay of G is governed by a time-dependent exponent for a wide range of r_\perp values, there must be analogous effects on the behavior of $S(\mathbf{q}, t)$. We defer detailed studies of the dynamic structure factor to the future, so that we can compare our theoretical predictions with our experimental results.

ACKNOWLEDGMENTS

We gratefully acknowledge the partial support of this work by KBN Grants Nos. 3T09A07212 and 2P03B12516.

-
- [1] A. Caillé, C. R. Seances Acad. Sci., Ser. B **274**, 891 (1972); also see the erratum in P.G. de Gennes, *The Physics of Liquid Crystals* (Oxford University Press, London, 1974), p. 336, Ref. [20].
- [2] J. Als-Nielsen, J. D. Litster, R. J. Birgeneau, M. Kaplan, C. R. Safinya, A. Lindgaard-Andersen, and S. Mathiesen, Phys. Rev. B **22**, 312 (1980); C. R. Safinya, D. Roux, G. S. Smith, S. K. Sinha, P. Dimon, N. A. Clark, and A. M. Bellocq, Phys. Rev. Lett. **57**, 2718 (1986).
- [3] R. Hołyst, D. J. Tweet, and L. B. Sorensen, Phys. Rev. Lett. **65**, 2153 (1990).
- [4] D. J. Tweet, R. Hołyst, B. D. Swanson, H. Stragier, and L. B. Sorensen, Phys. Rev. Lett. **65**, 2157 (1990).
- [5] R. Hołyst, Phys. Rev. A **44**, 3692 (1991).
- [6] V. M. Kaganer, B. I. Ostrovskii, and W. H. de Jeu, Phys. Rev. A **44**, 8158 (1991).
- [7] A. N. Shalaginov and V. P. Romanov, Phys. Rev. E **48**, 1073 (1993).
- [8] J. D. Shindler, E. A. L. Mol, A. Shalaginov, and W. H. de Jeu, Phys. Rev. Lett. **74**, 722 (1995).
- [9] E. A. L. Mol, J. D. Shindler, A. N. Shalaginov, and W. H. de Jeu, Phys. Rev. E **54**, 536 (1996).

- [10] N. Lei, C. R. Safinya, and R. F. Bruinsma, *J. Phys. II* **5**, 1155 (1995).
- [11] P. C. Martin, O. Parodi, and P. S. Pershan, *Phys. Rev. A* **6**, 2401 (1972).
- [12] G. F. Mazenko, S. Ramaswamy, and J. Toner, *Phys. Rev. Lett.* **49**, 51 (1982); *Phys. Rev. A* **28**, 1618 (1983).
- [13] G. Grinstein and R. A. Pelcovits, *Phys. Rev. Lett.* **47**, 856 (1981); *Phys. Rev. A* **26**, 915 (1982).
- [14] A. Poniewierski, R. Hołyst, A. C. Price, L. B. Sorensen, S. D. Kevan, and J. Toner, *Phys. Rev. E* **58**, 2027 (1998).
- [15] P. G. de Gennes and J. Prost, *The Physics of Liquid Crystals*, 2nd ed. (Clarendon, Oxford, 1993).
- [16] H.-Y. Chen and D. Jasnow, *Phys. Rev. E* **57**, 5639 (1998).
- [17] Y. Liao, N. A. Clark, and P. S. Pershan, *Phys. Rev. Lett.* **30**, 639 (1973).
- [18] A. C. Price, L. B. Sorensen, S. D. Kevan, J. Toner, A. Poniewierski, and R. Hołyst, *Phys. Rev. Lett.* (to be published).
- [19] P. Mach *et al.*, *J. Phys. II* **5**, 217 (1995).
- [20] P. Oswald (private communication); *J. Phys. (France)* **47**, 1091 (1986).
- [21] C. Baumann, J. P. Marcerou, J. Prost, and C. Rouillon, *Phys. Rev. Lett.* **54**, 1268 (1985).
- [22] S. Ramaswamy, J. Prost, W. Cai, and T. C. Lubensky, *Europhys. Lett.* **23**, 271 (1993).
- [23] R. Hołyst, *Phys. Rev. A* **46**, 6748 (1992).